Polymer 51 (2010) 877–882

Contents lists available at ScienceDirect

Polymer

journal homepage: www.elsevier.com/locate/polymer

Study of telechelic polyurethane with perfluoropolyether tails

Qingzeng Zhu [a], Charles C. Han [b,*]

[a] School of Chemistry and Chemical Engineering, Shandong University, Shanda Nanlu 27, Jinan 250100, China
[b] Beijing National Laboratory of Molecular Sciences, Joint Laboratory of Polymer Science and Materials, State Key Laboratory of Polymer Physics and Chemistry, Institute of Chemistry, CAS 2 Zhongguancun Bei Yi Jie, Beijing 100190, China

ARTICLE INFO

Article history:
Received 16 November 2009
Received in revised form
22 December 2009
Accepted 22 December 2009
Available online 11 January 2010

Keywords:
Telechelic polyurethane
Perfluoropolyether
Surface property

ABSTRACT

Well architectured polyurethanes containing fluorine are expected to be applied in medical devices as well as other fields. A telechelic polyurethane end-capped with perfluoropolyether segments was prepared from polyether glycol as a soft segment, 4, 4′-methylene-bis-(phenylisocyanate), and monofunctional perfluorinated oligomer. The telechelic polyurethane was studied by Fourier transform infrared spectroscopy (FTIR), gel permeation chromatography (GPC), differential scanning calorimetry (DSC), thermogravimetric analysis (TGA), X-ray photoelectron spectroscopy (XPS), contact angle and atomic force microscopy (AFM). XPS results indicated that the surface of the fluorine containing polyurethane was enriched with fluorine component. It exhibited a hydrophobic property with a water contact angle of 113°. The polyurethane terminated with perfluoropolyether segments showed a better thermal stability. A mechanism was proposed to explain thermal decomposition of polyurethanes. DSC results suggested that the tail-like perfluoropolyether segments would disrupt main chain packing, then raise crystallization potential barrier, and the perfluoropolyether segments did not affect the bulk microphase-separated structure.

1. Introduction

Polyurethanes have excellent and fine tuning properties. Fluorinated polyurethanes combine some virtues of polyurethane and fluorinated polymer, such as high thermal stability [1], good chemical resistance [2,3], attractive surface properties [4–7], and biocompatibility [8–10]. Some research works were devoted to well architectured polyurethane containing fluorine. Generally, fluorinated segments were incorporated into polyurethanes via fluorinated polyether or polyester diols as a soft segment [6,9,11–19], or fluorinated chain extenders [8,19–28], or fluorinated diisocyanates as a hard segment [19]. However, only a few studies were published on well architectured polyurethane end-capped with fluorinated segments. Fluorocarbon chain end-capped polyurethanes were designed and prepared as additives to modify polymer materials [29–35]. For instance, Tang et al. [29] prepared oligomeric polyurethanes end-capped with perfluorocarbon segments (CF_3–$(CF_2)_m$–CH_2CH_2OH, $m = 3$–17). The fluorinated polyurethanes were used as surface modifying macromolecules (SMM) to modify the surface of base poly(ester urethane). Khayet [31] used SMM to alter the surface chemistry of polyethersulfone membranes. Lee [32] synthesized a similar surface modifying agent and used it to modify UV cured polyurethane dispersion. Xie [33] prepared perfluorocarbon end-capped poly(carbonate urethane)s which were applied in a blend system. Until now, the effect of tail-like fluorinated segment on polyurethane has not been extensively studied.

In this article, a telechelic poly(ether urethane) (TFPU) which the linear molecular chains were end-capped with perfluoropolyether segments was synthesized and characterized. The effect of tail-like perfluoropolyether segments on properties of the telechelic polyurethane was discussed. In addition, the studies of multiform geometrical microstructured surfaces and electrospin fibre fabricated from these materials were published elsewhere [36,37].

2. Experimental section

2.1. Materials

Perfluorinated oligomer (PFOL, $CF_3CF_2CF_2O(CFCF_3CF_2O)_2CFCF_3$-$CH_2OH$) was kindly supplied by professor Fengling Qing (Shanghai Institute of Organic Chemistry, CAS). A commercially available 4, 4′-methylene-bis-(phenylisocyanate) (MDI) was supplied from Acros Organics. TERATHANE® 2000 polyether glycol (PEG, $M_n = 2000$ g mol^{-1}), 1,4-butanediol (CE), *N*,*N*-dimethylacetamide (DMAc), methanol and dimethylformamide (DMF) were purchased

* Corresponding author. Tel.: +86 531 88362866; fax: +86 531 88564464.
E-mail addresses: qzzhu@sdu.edu.cn (Q. Zhu), c.c.han@iccas.ac.cn (C.C. Han).

0032-3861/$ – see front matter © 2010 Elsevier Ltd. All rights reserved.
doi:10.1016/j.polymer.2009.12.033

Table 1
The composition, molecular weight of TFPU and PU.

Sample	Molar ratio of MDI:PEG:CE:PFOL	M_w ($\times 10^5$)	Polydispersity
PU	2.00:1.80:0.20:0.00	2.96	1.71
TFPU	2.00:1.80:0.19:0.02	2.18	1.94

from Aldrich. PEG was dehydrated under vacuum at 65 °C for 48 h before used. DMAc and 1,4-butanediol were distilled under vacuum and then dried over 4 Å molecular sieves.

2.2. Synthesis of PU and TFPU

The method for preparing TFPU was a two-step condensation reaction. The feed ratio of reactants is shown in Table 1. A typical procedure is described as follow: 5.0 g MDI was dissolved in DMAc (10.0 wt%) in a three-necked, round bottom flask under nitrogen atmosphere. 36.0 g PEG in DMAc (25.0 wt%) was subsequently added to the MDI solution at room temperature. The polymerization was carried out at 70–80 °C for 2 h. 0.16 ml 1,4-butanediol dissolved in DMAc were added as chain extenders. The chain extension reaction was continued for 2 h at 70–80 °C. The signal for free NCO groups appeared at 2270 cm^{-1} was monitored by a Fourier transform infrared spectroscopy (FTIR). Then 0.14 g PFOL was added drop by drop to the prepolymer solution and the reaction was kept for 4–6 h. Reaction completion was confirmed by the absence of FTIR absorption of the free NCO group. The resulting reactant was poured into deionized water. TFPU precipitated was dried in a vacuum oven at 60 °C. For purification, the TFPU was dissolved in DMAc again, and precipitated in a mixture of methanol and water to remove low molecular weight materials. The purified TFPU was washed with methanol and deionized water in turn, and dried at 60 °C under vacuum.

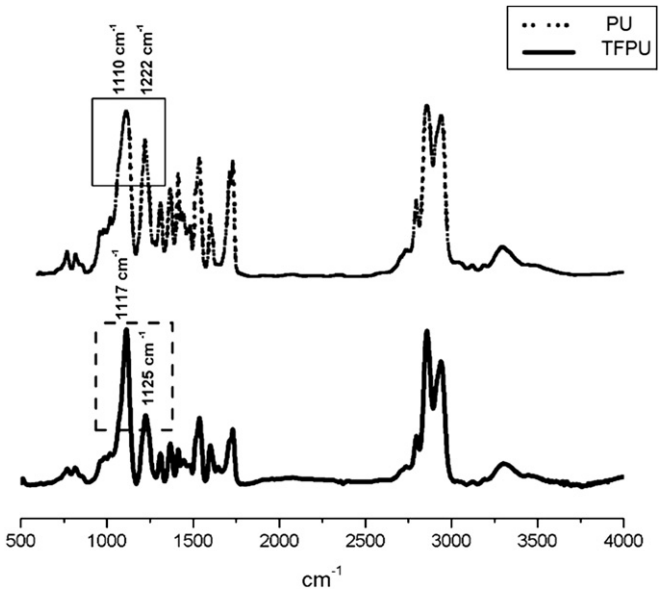

Fig. 1. FTIR spectra of PU (above) and TFPU (below).

In addition, polyurethane (PU) which has a similar structure was also synthesized for a comparison. The preparing process and reaction conditions of the PU were almost as same as those of the TFPU, only without PFOL added. The feed ratio of reactants was just slightly changed and shown in Table 1.

2.3. Characterization

Thin polymer films for XPS, contact angle and AFM studies were prepared by spin coating of a 10.0 wt% DMF solution onto glass

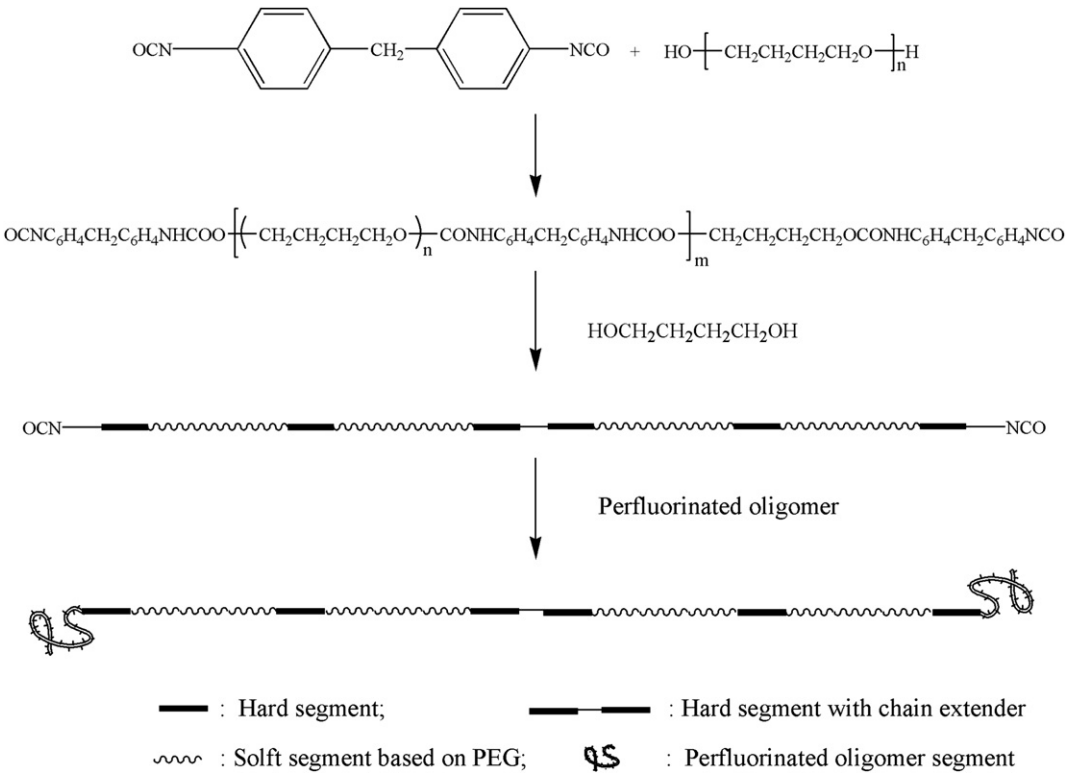

Scheme 1. Reaction route of TFPU copolymer.

Table 2
XPS data for TFPU.

Peaks	30°[a]			90°[a]		
	Binding energy	Norm area	[at]%[b]	Binding energy	Norm area	[at]%
F 1s	689.40 eV	0.04826	30.300	689.20 eV	0.05175	23.276
O 1s	532.60 eV	0.02210	13.877	532.55 eV	0.03193	14.361
N 1s	399.95 eV	0.00364	2.287	399.70 eV	0.00578	2.598
C 1s	285.00 eV	0.08526	53.536	284.85 eV	0.13287	59.764
F/C			0.57			0.39

[a] Take-off angle.
[b] [at]%: atom percent (F, O, N and C).

plates. The specimens were dried at 60 °C for 24 h, and further dried in a vacuum oven at 90 °C for 48 h to remove any residual solvent.

FTIR was performed to confirm the structure of the synthesized polymers with a Bruker Vertex-70 spectrometer (Germany) in the range 4000–400 cm^{-1}. Each sample for infrared analysis was prepared by casting the polymer onto a clean potassium bromide disc from a single drop of 1.0 wt% DMF solution. These samples were put into an oven at 90 °C for 48 h under vacuum to completely remove the solvent.

Thermal transitions were measured using a differential scanning calorimetry (DSC, METLLER Toledo DSC822^e). Samples were prepared by casting DMF solution into the pans. After evaporation of the solvent, the specimens were dried at 90 °C for 48 h in a vacuum oven to remove residual solvent. Sample weight was about 3.0–8.0 mg. Before scanning, the samples were first heated to 200 °C and maintained at 200 °C for 3.0 min to eliminate thermal history. The samples were cooled to −70 °C at a rate of 10 °C/min and held at −70 °C for 5.0 min, followed by reheating to 200 °C at a rate of 10 °C/min. All operations were carried out under a nitrogen environment. The midpoint with half of the total change in specific heat capacity in the curve was characterized as glass transition temperature (T_g).

Thermogravimetric analysis (TGA) was performed using a Pyris 1 (PerkinElmer). The samples (6.0–10.0 mg) were heated from room temperature to 700 °C under nitrogen at a rate 10 °C/min.

Gel permeation chromatography (GPC) equipped with a 515 system (Waters), a 2410 refractive index and two Styragel gel columns, calibrated with narrow molecular weight polystyrene standards, was used to estimate the molecular weights of polymers synthesized. The mobile phase was DMF. Sample concentration was about 3.0 mg/ml and the injection volume was 100 μl. The flow rate was kept at 1.000 ml/min and the temperature of system was 40 °C.

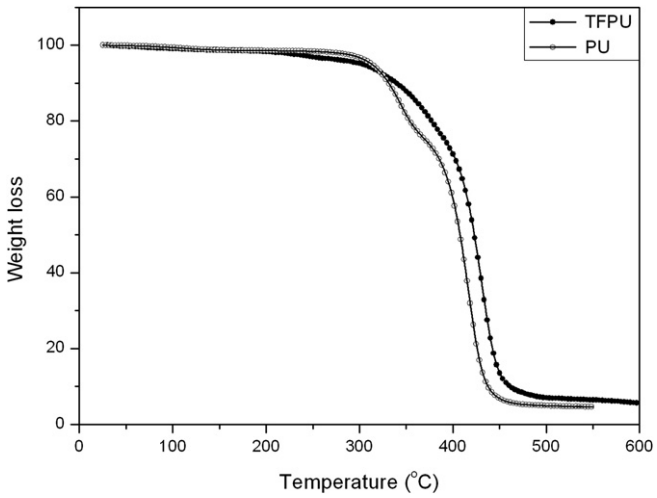

Fig. 3. TGA thermographs of TFPU and PU (10 °C/min, N_2).

X-ray photoelectron spectroscopy (XPS) data were obtained with an ESCALab220i-XL electron spectrometer from VG Scientific using 300 W AlK_α radiation. The binding energies were referenced to the C1s line at 284.8 eV from adventitious carbon. XPS results were obtained on the air-facing side of the specimen films.

The atomic force microscope (AFM) measurements were performed on the JPK NanoWizard® AFM system (JPK Instruments AG) at room temperature, using Olympus OMCL-RC 800 PSA cantilevers. In contact mode, the topographic and phase data were recorded simultaneously.

The static contact angle was measured using a sessile drop method. A water drop of 5.0 μL was used. Each water contact angle (WCA) was an average value of at least five measurements on different locations of the surface.

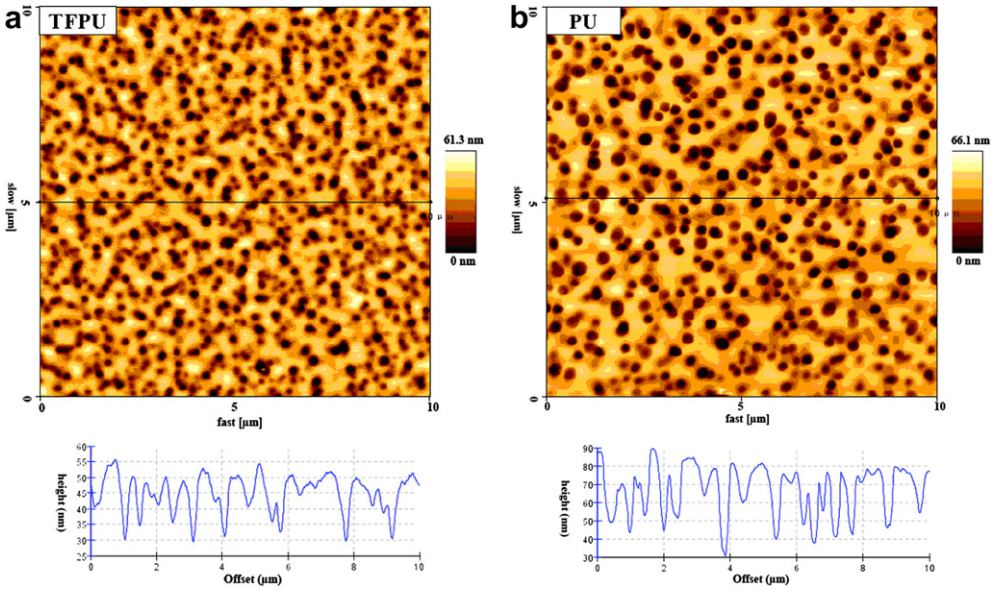

Fig. 2. Height images and profile inspecting lines of TFPU (a) and PU (b) by AFM.

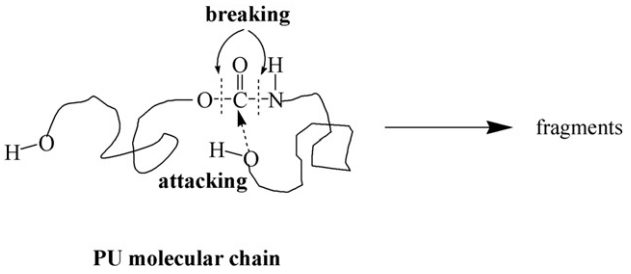

Scheme 2. Schematic thermal decomposition mechanism of PU.

3. Results and discussion

3.1. The macromolecular architecture design

TFPU was prepared from PEG as a soft segment, MDI and monofunctional perfluorinated oligomer using a two-step condensation reaction. Its linear main chains were terminated with perfluoropolyether segments (Scheme 1). PU had a same structure only without perfluoropolyether tails. Table 1 lists the molecular weights and polydispersities of TFPU and PU obtained by GPC. The weight-average molecular weights (M_w) of TFPU and PU are close.

3.2. IR

Fig. 1 shows the FTIR spectra of TFPU and PU. The absorption bands at 2750–3000 cm^{-1} (CH stretching vibrations), at 1720 cm^{-1} (C═O stretching vibrations), and at 1540 cm^{-1} (NH in plane bending), were observed in the spectra. There are phenyl absorption bands at 1600 cm^{-1}, 820 cm^{-1} and 768 cm^{-1}. The two strong absorption at 1222–1225 cm^{-1} and 1110–1117 cm^{-1} are assigned to the C–O–C (stretching vibrations in ester bond). However, ether bond antisymmetric vibration also occurs at 1110 cm^{-1}. C–F exhibits symmetric vibration near 1110 cm^{-1} [38]. Compared the bands at 1110–1117 cm^{-1} with the bands at 1222–1225 cm^{-1} in the two spectra, it is clear that the intensity of the band at 1117 cm^{-1} in TFPU spectrum grew up. This arises from the contribution of C–F bonds.

3.3. Surface properties

Films were prepared by spin coating of a 10.0% (w/v) DMF solution of TFPU on glass substrates. Angle-dependent XPS was employed to quantify the surface composition. Generally, the take-off angle represents the detection depth. 30° is near the surface 5 nm and 90 °C is around 10 nm away from the surface. The XPS results were summarized in Table 2. F (1s) peak was observed at 689 eV. The fluorine atomic percentage (C, O, F and N) calculated from the stoichiometric values of the reactants in the TFPU bulk is 0.16%. XPS analysis showed that the fluorine atomic percentage was 23.3% at the depth of 10 nm surface, and 30.3% at the depth of 5 nm surfaces. F/C atomic ratio at the depth of 5 nm was 0.57, which was higher than that (0.39) at the depth of 10 nm surface. Considering 59.0% calculated fluorine atomic ratio in PFOL, it suggested that more perfluoropolyether segments enriched to the uppermost 5 nm surface of TFPU.

As we know, the surface enriched with fluorine is attributed to the low surface free energy of the fluorine sequences, which possesses a thermodynamic driving force for migration to the polymer–air interface. Further more, only one side of the perfluorinated segments were anchored in the telechelic polyurethane, these tail-like perfluoropolyether segments could have a higher mobility than those embedded in main chain. So these perfluoropolyether segments can migrate to the surface more easily.

Surface dewetting behaviors also indicated the surface components change of TFPU. Static water contact angles on the PU film was 85 ± 2.3°. However, TFPU show a hydrophobic property with a static water contact angles of 113 ± 1.2°, comparable to contact angle values obtained for pure Teflon [39]. AFM images showed that the TFPU and PU films had a similar surface structure and roughness (Fig. 2). So the hydrophobicity of TFPU arises from the high fluorine content on its surface.

3.4. TGA

The thermal stability of TFPU and PU were investigated by TGA under nitrogen. As shown in Fig. 3, the temperature of initial 10% weight loss for TFPU and PU occurred at 340 °C and 335 °C respectively. In the range of 20–80% weight loss, the thermal decomposition temperature of TFPU is about 15 °C higher than that of PU at the same weight loss. This indicated that TFPU had a higher thermal stability. Usually, PU molecular chains are terminated with hydroxyls which come from diols. Under the higher temperature, the hydroxyls might attack the urethane bonds via an intermolecular or intramolecular reactions, and break the main chain (Scheme 2). In that case, the thermal decomposition of PU molecular chains will become easily. It can be understood that TFPU which has no active hydroxyls at the end of molecular chains will have a higher thermal stability.

3.5. Crystallization

Comparison of DSC traces was done for the investigation of thermal properties of TFPU. PEG was performed to clarify the

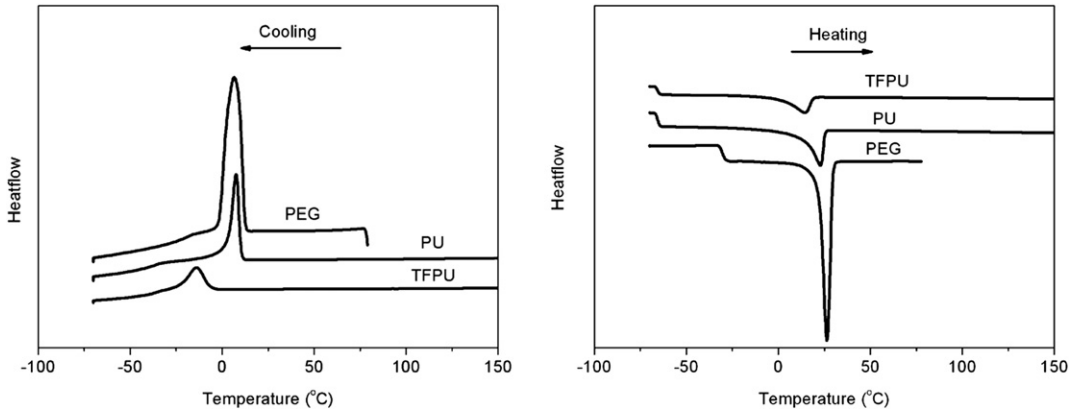

Fig. 4. The DSC thermogrames of PEG, PU and TFPU on cooling the melt and in the second heating run (10 °C/min, N_2).

Table 3
DSC data for PEG, PU and TFPU from cooling and reheating scans.

Sample	Cooling scan			Reheating scan			
	T_c(°C)	ΔH_c (J/g)	X (%)[a]	T_g(°C)	T_m(°C)	ΔH_m (J/g)	X (%)
PEG	6.5	97.4	100	−31.2	26.5	−99.6	100
PU	7.6	36.0	37.0	−65.0	22.9	−42.7	42.9
TFPU	−14.0	25.0	25.7	−65.0	14.5	−31.4	31.5

[a] X (degree of soft segment crystallinity) in terms of the ratio of the crystallization: $X = \Delta H/\Delta H_0$, where ΔH_0 is the crystallization or melting enthalpy of pure PEG. ΔH represents ΔH_m or ΔH_c.

thermal behaviors of soft segments in PU and TFPU. Fig. 4 shows the cooling and reheating scans respectively. The thermal transitions observed in TFPU and PU include an exothermic crystallization peak in the cooling scan, and a distinct glass transition and an endothermic melting peak in the reheating scans. The crystallization temperature (T_c), T_g, melting temperature (T_m), melting enthalpy (ΔH_m) and recrystallization enthalpy (ΔH_c) obtained from DSC scans are summarized in Table 3. It indicated that TFPU was a semicrystalline copolymer.

The thermogram of PEG shows a larger exothermic peak at 6.5 °C on the cooling scan and a larger endothermic peak at 26.5 °C on the reheating scan. The ΔH_m and ΔH_c of PEG calculated from the DSC peaks were −99.6 J/g and 97.4 J/g respectively. PU shows an exothermic peak at 7.6 °C and an endothermic peak at 22.9 °C. The T_c and T_m of PEG and PU are approximate. However, compared with PEG, the ΔH_c (36.0 J/g) and ΔH_m (−42.7 J/g) of PU decreased. The soft PEG segments in polyurethane form the main crystalline structure. If we define the degree of soft segment crystallinity X ($X = \Delta H/\Delta H_0$, where ΔH_0 is the crystallization or melting enthalpy of pure PEG, ΔH represents ΔH_m or ΔH_c) in terms of the ratio of the crystallization. As shown in Table 3, PU gave a lower degree of crystallinity. This can be mainly attributed to the disruption of soft segments crystal structure at a certain extent by hard segments and coiled macromolecules.

Compared with PU, both the endothermic peak and the exothermic peak of TFPU shifted to lower temperature. The T_c and T_m of TFPU were −14.0 °C and 14.5 °C respectively. At the same time, the ΔH_m and ΔH_c of TFPU decrease further (see Table 3). Tail-like perfluoropolyether segments in the polyurethane chains possess highly migrating property. The migration behavior of the low surface energy segments in the bulk will disrupt main chain packing, and then raise crystallization potential barrier. So crystallization of TFPU needs a more lower temperature. This was clearly verified in Fig. 4. Compared with that of PU, the crystallization peak of TFPU on the cooling curve shifted to low temperature 21.6 °C. The relative unperfect crystallization structure due to the disruption of perfluoropolyether segments made T_m and ΔH_m of TFPU decrease noticeably.

Table 3 also indicated that all the crystallization enthalpies of PEG, PU and TFPU in the cooling scans were less than their corresponding melting enthalpies in the reheating scans. This can be attributed to a dynamic crystallization process. Under the lower temperature and extending time conditions, more crystal would be formed. So the melting enthalpies in the reheating scans increased.

3.6. Glass transition

The step-like changes of PEG, PU and TFPU were observed distinctly at −31.2 °C, −65.0 °C and −65.0 °C on their reheating scans respectively (Fig. 4). PEG is an oligomer with higher crystallinity. It presented a higher T_g. TFPU and PU were copolymers with M_w of 2.96×10^5 and 2.18×10^5 respectively. The longer molecular chain and lower crystallinity of TFPU and PU increase main chain flexibility. So this made their glass transition happen at lower temperature. TFPU and PU show a same T_g (−65.0 °C). This result indicated that the tail-like perfluoropolyether segments in the linear polyurethane chains did not affect the bulk microphase-separated structure.

4. Conclusion

A telechelic polyurethane end-capped with perfluoropolyether segments was prepared from polyether glycol, MDI and monofunctional perfluorinated oligomer. The tail-like perfluoropolyether segments have a higher mobility for migration to the surface. The novel fluorinated polyurethane show a similar surface hydrophobic property with pure Teflon. The hydrophobicity arises from the high fluorine content on its surface. Compared with general polyurethane, the polyurethane terminated with perfluorinated segments exhibited a higher thermal stability. We propose that the hydroxyl groups at the end of polyurethane molecular chains will attack and break the urethane bonds via intermolecular or intramolecular reactions in the heating process. So the hydroxyl groups can induce thermal decomposition of main chains. The highly migrating behavior of perfluorinated segments disrupted main chain packing, then raised their crystallization potential barrier. So crystallization happened at a lower temperature. It also made the crystallization and melting enthalpies of the fluorinated polyurethane decrease noticeably. Our results suggested that the tail-like perfluoropolyether segments did not affect the bulk microphase-separated structure.

Acknowledgements

The authors are grateful for the financial support of Natural Science Foundation of China (No. 20404006), Shandong Province Natural Science Foundation (No. ZR2009BM038) and National "973" Project (No. 2009CB930103).

References

[1] Chapman TM. J Polym Sci Part A Polym Chem 1989;27:1993.
[2] Tonelli C, Ajroldi GJ. J Appl Polym Sci 2003;87:2279.
[3] Chattopadhyay DK, Raju KVSN. Prog Polym Sci 2007;32:352.
[4] Chapman TM, Benrashid R, Marra KG, Keener JP. Macromolecules 1995;28:331.
[5] Schmidt DL, Coburn CE, Dekoven BM, Potter GE, Mayers GF, Fischer DA. Nature 1994;368:39.
[6] Kim YS, Lee JS, Ji Q, McGrath JE. Polymer 2002;43:7161.
[7] Janine MO, Toby MC, William RW, Ron J. J Polym Sci Part A Polym Chem 1999;37:3441.
[8] Chen KY, Kuo JF. Macromol Chem Phys 2000;201:2676.
[9] Guerra RSD, Lelli L, Tonelli C, Trombetta T, Cascone MG, Taveri M, et al. J Mater Sci Mater Med 1994;5:452.
[10] Yoon SC, Ratner BD. Macromolecules 1986;19:1068.
[11] Tonelli C, Trombetta T, Scicchitano M, Castiglioni G. J Appl Polym Sci 1995;57:10312.
[12] Ho T, Wynne KJ. Macromolecules 1992;25:3521.
[13] Delucchi M, Turri S, Barbucci A, Bassi M, Novelli S, Cerisola G. J Polym Sci Part B Polym Phys 2002;40:52.
[14] Honeychuck RV, Ho T, Wynne KJ, Nissan RA. Chem Mater 1993;5:1299.
[15] Tamareselvy K, Venkatarao K, Kothandaraman H. J Polym Sci Part A Polym Chem 1990;28:2679.
[16] Turri S, Levi M, Trombetta T. J Appl Polym Sci 2004;93:136.
[17] Ge Z, Zhang XY, Dai JB, Li WH, Luo YJ. Eur Polym J 2009;45:530.
[18] Tonelli C, Ajroldi G, Marigo A, Marego C, Turturro A. Polymer 2001;42:9705.
[19] Takakura T, Kato M, Yamabe M. Makromol Chem 1990;191:625.
[20] Yoon SC, Ratner BD. Macromolecules 1988;21:2392.
[21] Tan H, Guo M, Du RN, Xie XY, Li JH, Zhong YP, et al. Polymer 2004;45:1647.
[22] Wang LF. Polymer 2007;48:894.
[23] Lin YH, Chou NK, Chang CH, Wang SS, Chu SH, Hsieh KH. J Polym Sci Part A Polym Chem 2007;45:3231.
[24] Tan H, Li JH, Guo M, Du RN, Xingyi Xie, Zhong YP, et al. Polymer 2005;46:7230.
[25] Tan H, Xie XY, Li JH, Zhong YP, Fu Q. Polymer 2004;45:1495.
[26] Kajiyama T, Takahara A. J Biomater Appl 1991;6:42.
[27] Yoon SC, Sung YK, Ratner BD. Macromolecules 1990;23:4351.
[28] Wang LF. Eur Polym J 2005;41:293.
[29] Tang YW, Santerre JP, Labow RS, Taylor DG. Biomaterials 1997;18:37.

[30] Matsuura T, Santerre JP, Narbaitz RM, Pham V, Fang Y, Mahmud H, Baig F. US Patent, US 5594966; 1999.
[31] Khayet M, Suk DE, Narbaitz RM, Santerre JP, Matsuura T. J Appl Polym Sci 2003;89:2902.
[32] Lee MH, Jang MK, Kim BK. Eur Polym J 2007;43:4271.
[33] Xie XY, Tan H, Li JH, Zhong YP. J Biomed Mater Res Part A 2008;84:30.
[34] Chen Z, Ward R, Tian Y, Eppler AS, Shen YR, Somorjai GA. J Phys Chem B 1999;103:2935.
[35] Xie QD, Fan GQ, Zhao N, Guo XL, Xu J, Dong JY, et al. Adv Mater 2004;16: 1830.
[36] Wu WL, Zhu QZ, Qing FL, Han CC. Langmuir 2009;25:17.
[37] Wu WL, Yuan GC, He AH, Han CC. Langmuir 2009;25:3178.
[38] Richard AN. Interpreting infrared, Raman, and nuclear magnetic resonance spectra. San Diego: Academic Press; 2001.
[39] Brandrum J, Immugut EA. Polymer handbook. 3rd ed. New York: John Wiley & Sons; 1989.